

# A Five-Membered Ru<sub>5</sub> Ring in a Hexagonal La<sub>14</sub> Cage: The La<sub>14</sub>Cl<sub>20</sub>Ru<sub>5</sub> Structure

Chong Zheng,<sup>\*,†</sup> Jürgen Köhler,<sup>\*,‡</sup> Hansjürgen Mattausch,<sup>‡</sup> Constantin Hoch,<sup>‡</sup> and Arndt Simon<sup>‡</sup>

<sup>†</sup>Department of Chemistry and Biochemistry, Northern Illinois University, DeKalb, Illinois 60115, United States

<sup>‡</sup>Max-Planck-Institut für Festkörperforschung, Heisenbergstrasse 1, D-70569 Stuttgart, Germany

**S** Supporting Information

**ABSTRACT:** The title compound features a five-membered Ru<sub>5</sub> ring embedded in a La<sub>14</sub> hexagonal wheel-like cage, an incommensurate combination of the two building units. A formal electron partition of (La<sup>3+</sup>)<sub>14</sub>(Cl<sup>-</sup>)<sub>20</sub>(Ru<sub>5</sub>)<sup>22-</sup> results in a (Ru<sub>5</sub>)<sup>22-</sup> ring isoelectronic to (Cd<sub>5</sub>)<sup>2-</sup>. However, computational studies show that there is significant electron back-donation from the Ru<sub>5</sub> ring to the La<sub>14</sub> wheel. This interaction strongly stabilizes the Ru<sub>5</sub> ring. The resistivity and magnetic susceptibility of the compound have also been investigated.

Pentagonal rings formed by the main-group elements are common in chemistry. These include the cyclopentadienyl anion and its Si, Ge, P, and As analogues.<sup>1–6</sup> However, five-membered transition-metal rings are extremely rare, if at all existing. Theoretical studies by Hoffmann and coworkers have suggested the possibility of their structural stability for certain electron counts.<sup>7</sup> Perhaps a suitable surrounding matrix can provide the geometric confinement and electronic requirement for their existence. The chemistry of reduced rare-earth (RE) metal halides can provide such a platform for synthesis, as it is extremely rich and versatile. The RE metal framework can accommodate endohedral atoms ranging from the light atoms H and B to heavy ones such as Au and Pb.<sup>8–20</sup> The structures of these halides are invariably based on simple RE<sub>6</sub> trigonal prisms or octahedra, which can be condensed into one-dimensional chains, two-dimensional sheets, and three-dimensional networks to provide a desirable environment for such metal rings. In this contribution, we report the synthesis of the compound La<sub>14</sub>Cl<sub>20</sub>Ru<sub>5</sub>, in which a five-membered Ru<sub>5</sub> ring is stabilized by a hexagonal La<sub>14</sub> wheel-like cage [the detailed synthesis and crystal structure determination procedures can be found in the Supporting Information (SI)]. The cage has hexagonal symmetry and thus is incommensurate with the five-membered Ru<sub>5</sub> ring. Computational analysis was therefore carried out to explore the origin and the structural stability of the La<sub>14</sub>–Ru<sub>5</sub> motif.

The crystal structure of La<sub>14</sub>Cl<sub>20</sub>Ru<sub>5</sub> contains hexagonal La<sub>14</sub> wheels (Figure 1a). Each wheel is assembled from two La-centered La<sub>6</sub> hexagons, one on each side of the Ru<sub>5</sub> ring, which are rotated with respect to each other by ca. 30 degrees. The hexagons are slightly distorted, with the lengths of the six sides ranging from 3.96 to 4.30 Å. The seven La atoms on each side of the wheel lie almost in a plane, with a maximum deviation from the plane of ca. 0.5 Å. The two hexagons are connected by

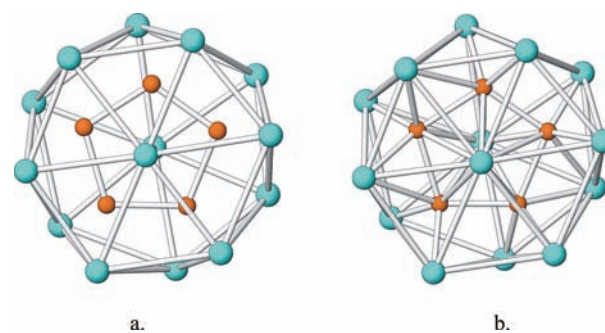


**Figure 1.** (a) La<sub>14</sub>Ru<sub>5</sub> wheel in the La<sub>14</sub>Cl<sub>20</sub>Ru<sub>5</sub> structure (La in blue, Ru in orange). (b) Coordination of Ru in the La<sub>14</sub>Ru<sub>5</sub> wheel.

12 La–La bonds on the cage sides whose lengths range from 3.75 to 4.16 Å. The two central La atoms in the hexagons are connected at a distance of 3.91 Å. The wheel can also be considered as constructed from 12 face-sharing La<sub>4</sub> tetrahedra. However, these tetrahedra need to distort to have equal sizes, as otherwise one side of the wheel would have regular tetrahedra and the other “squeezed” ones.

The hexagonal La<sub>14</sub> wheel encloses a five-membered Ru<sub>5</sub> ring. Ideally, one would expect a Ru<sub>6</sub> hexagon to be fitted into the wheel, as every other tetrahedral void would then be occupied. However, it is well-known that transition-metal endohedrals prefer to occupy octahedral holes in reduced RE metal halides. Thus, the Ru atoms shift from the centers of the tetrahedra to form a five-membered ring. In doing so, within the sum of the covalent radii of La and Ru (La 2.07 Å, Ru 1.46 Å),<sup>21</sup> each Ru atom is coordinated to five La atoms in a highly distorted square-pyramidal mode, with the La–Ru contacts ranging from 2.46 to 3.34 Å. With the two additional Ru–Ru bonds, each Ru atom is seven-coordinate (Figure 1b). The Ru<sub>5</sub> ring is almost regular, with Ru–Ru distances varying from 2.67 to 2.72 Å, which is only slightly longer than that in Ru metal (2.65 Å), and the maximum deviation of the Ru atoms from the five-membered-ring plane is ca. 0.015 Å. Extended Hückel (EH) calculations indicated that the Ru<sub>5</sub> ring can rotate about the central axis inside the La<sub>14</sub> cage with very little barrier.

There are two such La<sub>14</sub>Ru<sub>5</sub> wheels in the unit cell. These are connected via the central La atoms in the *a* direction, with the La–La contacts being 4.22 Å on both sides (Figure 2a). The shortest side contacts between the wheels are 4.23 Å, which is

Received: December 6, 2011

Published: February 22, 2012

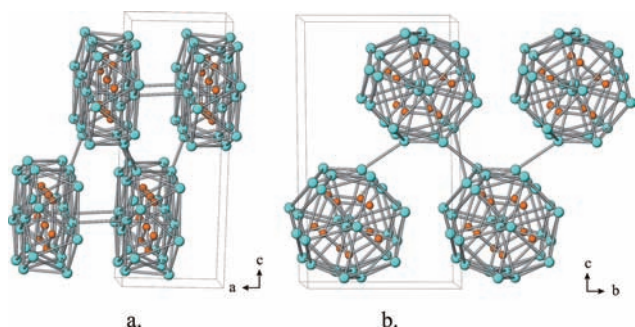


**Figure 2.** Connection of the  $\text{La}_{14}\text{Ru}_5$  wheels in (a) the  $a$  direction and (b) the  $b$  direction.

larger than the sum of the covalent radii of La. Thus, these wheels are mainly connected by sharing of Cl ligands in all directions. All Cl atoms are shared by two to four La atoms (see Figure S4 in the SI). Several Cl atoms, in particular Cl, Cl2, Cl1, Cl4, and Cl0 (see Table S2 in the SI), choose two or more chemically similar positions and form equivalent La–Cl bonds (see Figures S3 and S5 in the SI). Thus, there are statistical disorders at these positions.

A formal electron partitioning of  $(\text{La}^{3+})_{14}(\text{Cl}^-)_{20}(\text{Ru}_5)^{22-}$  leaves the  $(\text{Ru}_5)^{22-}$  ring isoelectronic to  $(\text{Cd}_5)^{2-}$ . An alternative description is  $(\text{La}^{2+})_{14}(\text{Cl}^-)_{20}(\text{Ru}_5)^{8-}$ , in which each La is in the 2+ charge state, giving a maximum number of electrons in the La framework (one per La atom, reducing it from 3+ to 2+).<sup>22</sup> Between these two extremes is still another scheme,  $(\text{La}^{3+})_{14}(\text{Cl}^-)_{20}(\text{Ru}^{2-})_5 \cdot 12e^-$ , in which the 12 excess electrons are distributed in metal–metal bonding within the La and Ru metal atom framework. Our detailed analyses based on EH calculations support the last one. First, our computational results for the  $\text{Ru}_5$  ring indicated that the five 4d orbitals of Ru are filled and lie low in energy (Figure S6). The symmetry-adapted cyclopentadienoid Ru 5s orbitals come next. When the  $\text{Ru}_5$  ring is incorporated in the  $\text{La}_{14}$  cage, the Ru 5s and 5p states are pushed up further, well above the Fermi level, through interactions with the lower La 5d states (Figure S7). In the EH density of states (DOS) calculated for the  $\text{La}_{14}\text{Cl}_{20}\text{Ru}_5$  structure (Figure 3), the corresponding Ru 4d states lie in the

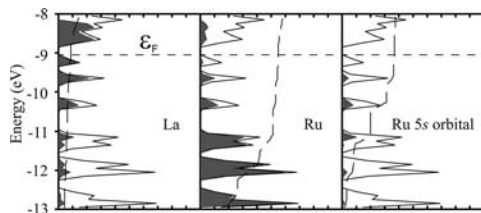


**Figure 3.** EH DOS plot. The solid curves represent the total DOS, and the shaded areas and dashed curves correspond to specific contributions and their integrated values, respectively. The horizontal dotted lines indicate the Fermi level.

energy range of  $-11$  to  $-14$  eV, well below the Fermi energy. Therefore, the Ru–Ru bonding and antibonding interactions compensate for each other, and the 10 4d electrons of Ru may be regarded as “pseudo-core” electrons. The bonding interactions below the Fermi level are mainly due to interactions of the Ru 5s and 5p orbitals with the La 5d states.

Figures 3 and 4 show the EH DOS and crystal orbital overlap population (COOP) curves, respectively. In the DOS plot, the states above the Fermi level are all La 5d. From the Fermi level

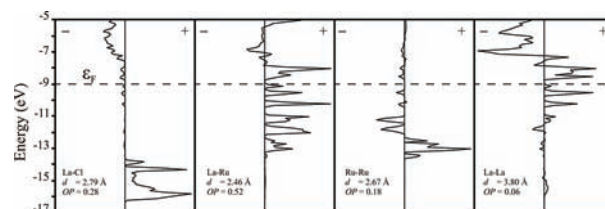


**Figure 4.** EH COOP curves of representative bonds in  $\text{La}_{14}\text{Cl}_{20}\text{Ru}_5$ . The + regions denote the bonding areas and the – regions denote the antibonding areas. The bond type, bond length ( $d$ ), and integrated overlap population (OP) up to the Fermi level are indicated in each panel.

downward to  $-14$  eV, the states are mostly Ru 4d. As can be seen in the figure, less than 25% of the Ru 5s states are occupied. These states are in the Ru 4d region because of the aforementioned mixing. They contribute to Ru–Ru antibonding, as shown in the COOP plot, and therefore are not the symmetry-adapted cyclopentadienoid Ru 5s states. The COOP curves show that all states below the Fermi level contribute to mostly La–Cl, La–Ru, and La–La bonding. However, there is significant Ru–Ru antibonding character below the Fermi level because of the  $d^{10}$ – $d^{10}$  interactions between the  $\text{Ru}^{2-}$  species. However, the antibonding contribution is less than the bonding one, leading to a net positive overlap population of ca. 0.18 that indicates an overall Ru–Ru bonding contribution from all states below the Fermi level. As can be seen from Figure S8, the Ru 5p states are mainly unoccupied and only a small amount lies below the Fermi level. Obviously the anionic Ru atoms in  $\text{La}_{14}\text{Cl}_{20}\text{Ru}_5$  do not behave like atoms of a p metal, as found for various other anionic heavy late-transition-metal atoms in polar intermetallic compounds.<sup>23</sup>

According to our linear muffin-tin orbital (LMTO) band structure calculations,  $\text{La}_{14}\text{Cl}_{20}\text{Ru}_5$  is a small-band-gap semiconductor with a band gap of ca. 0.3 eV (Figure S9). For comparison, the band gap from the resistivity measurement was 0.11 eV (Figure S10). The EH method also predicts semiconducting behavior of the compound, with a band gap of ca. 0.5 eV.

Magnetic susceptibility measurements on  $\text{La}_{14}\text{Cl}_{20}\text{Ru}_5$  revealed that the compound is nonmagnetic with a trace amount of a magnetic impurity (Figure S11), in agreement with the prediction of the EH and LMTO calculations that the electronic structure of the compound has a closed-shell configuration. The resistivity measured in the temperature range from 20 to 300 K indicated that the compound is a semiconductor, as expected from the discrete clusters interconnected via nonmetal Cl atom bridges at all surrounding corners.<sup>24</sup>

## ■ ASSOCIATED CONTENT

### Supporting Information

Synthesis procedure, selected crystallographic data (CIF), computational details, and additional figures. This material is available free of charge via the Internet at <http://pubs.acs.org>.

## ■ AUTHOR INFORMATION

### Corresponding Author

[czheng@niu.edu](mailto:czheng@niu.edu); [j.koehler@fkf.mpg.de](mailto:j.koehler@fkf.mpg.de)

### Notes

The authors declare no competing financial interest.

## ■ ACKNOWLEDGMENTS

C.Z. acknowledges the continuous support of Max-Planck Gesellschaft which makes visit to MPI possible.

## ■ REFERENCES

- (1) Schnering, H. G.; Nesper, R.; Curda, J.; Tebbe, K.-F. *Angew. Chem., Int. Ed. Engl.* **1980**, *19*, 1033.
- (2) Böhm, M. C.; Ramirez, R.; Nesper, R.; Schnering, H. G. *Phys. Rev. B* **1984**, *30*, 4870.
- (3) Nesper, R.; Schnering, H. G.; Curda, J. *Chem. Ber.* **1986**, *119*, 3576.
- (4) Frank, U.; Müller, W. Z. *Naturforsch., B* **1975**, *30*, 313.
- (5) Bai, J.; Virovets, A. V.; Scheer, M. *Angew. Chem., Int. Ed.* **2002**, *41*, 1737.
- (6) Gascoin, F.; Sevov, S. C. *Inorg. Chem.* **2002**, *41*, 2292.
- (7) Tang, H.; Hoffman, D. M.; Albright, T. A.; Deng, H.; Hoffmann, R. *Angew. Chem., Int. Ed. Engl.* **1993**, *32*, 1616.
- (8) Simon, A.; Mattausch, H.; Müller, G. J.; Bauhofer, W.; Kremer, R. K. *Handb. Phys. Chem. Rare Earths* **1991**, *15*, 191.
- (9) Mattausch, H.; Simon, A. *Angew. Chem., Int. Ed.* **1998**, *37*, 499.
- (10) Mattausch, H.; Oeckler, O.; Simon, A. *Inorg. Chim. Acta* **1999**, *289*, 174.
- (11) Warkentin, E.; Simon, A. *Rev. Chim. Miner.* **1983**, *20*, 488.
- (12) Nagaki, D.; Simon, A.; Borrmann, H. J. *Less-Common Met.* **1989**, *156*, 193.
- (13) Dorhout, P. K.; Payne, M. W.; Corbett, J. D. *Inorg. Chem.* **1991**, *30*, 4960.
- (14) Llusar, R.; Corbett, J. D. *Inorg. Chem.* **1994**, *33*, 849.
- (15) Hughbanks, T.; Rosenthal, G.; Corbett, J. D. *J. Am. Chem. Soc.* **1986**, *108*, 8289.
- (16) Hughbanks, T.; Corbett, J. D. *Inorg. Chem.* **1988**, *27*, 2022.
- (17) Hughbanks, T.; Corbett, J. D. *Inorg. Chem.* **1989**, *28*, 631.
- (18) Meyer, G.; Wickleder, M. S. *Handb. Phys. Chem. Rare Earths* **2000**, *28*, 53.
- (19) Corbett, J. D. *J. Chem. Soc., Dalton Trans.* **1996**, 575.
- (20) Simon, A.; Mattausch, H.; Ryazanov, M.; Kremer, R. K. *Z. Anorg. Allg. Chem.* **2006**, *632*, 919.
- (21) Cordero, B.; Gómez, V.; Platero-Prats, A. E.; Revés, M.; Echeverría, J.; Cremades, E.; Barragán, F.; Alvarez, S. *Dalton Trans.* **2008**, 2832.
- (22) Zheng, C.; Oeckler, O.; Mattausch, H.; Simon, A. *Z. Anorg. Allg. Chem.* **2001**, *627*, 2151.
- (23) (a) Whangbo, M.-H.; Lee, C.; Köhler, J. *Angew. Chem.* **2006**, *118*, 7627; *Angew. Chem., Int. Ed.* **2006**, *45*, 7465. (b) Köhler, J.; Whangbo, M.-H. *Solid State Sci.* **2008**, *10*, 449. (c) Köhler, J.; Whangbo, M.-H. *Chem. Mater.* **2008**, *20*, 2751. (d) Whangbo, M.-H.; Lee, C.; Köhler, J. *Eur. J. Inorg. Chem.* **2011**, 3841.
- (24) Simon, A. *Angew. Chem., Int. Ed. Engl.* **1988**, *27*, 159.